

A disordered insulator in an optical lattice

M. Pasienski, D. McKay, M. White and B. DeMarco*

Disorder can profoundly affect the transport properties of a wide range of quantum materials. At present, significant disagreement exists regarding features of the disordered Bose-Hubbard model, which is used to study disorder in strongly correlated bosonic systems^{1,2}. Here, by measuring transport³ in a disordered optical lattice⁴, we discover a disorder-induced superfluid-to-insulator transition in this system, in quantitative agreement with a predicted superfluid-Bose-glass transition from recent numerical simulations⁵. Both the superfluid-to-insulator transition and correlated changes in the atomic quasimomentum distribution—which verify a simple model for the interplay of disorder and interactions in this system—are phenomena new to the unit-filling regime explored in this work. We find that increasing disorder strength generically leads to greater dissipation, excluding predictions of a disorder-induced or ‘re-entrant’ superfluid. Whereas the absence of a re-entrant superfluid may be explained by finite temperature, the measured bounds on entropy strongly constrain theory.

A wide range of sophisticated theoretical approaches applied to determine the ground-state phase diagram of the disordered Bose-Hubbard (DBH) model have reached inconsistent conclusions (see refs 1,2 and 6 for an overview and refs 5,7–10 for recent results). Precisely how insulating phases arise as microscopic parameters are varied is at present a subject of intense debate, particularly for three-dimensional systems. Resolving these issues by comparison to measurements on solids is complicated by incomplete knowledge of the physical disorder and the influence of other degrees of freedom, such as lattice distortions and long-range electronic interactions. In particular, the Bose-glass phase—a compressible, gapless insulator first discussed in ref. 11—has yet to be unambiguously observed in an experiment (see refs 12 and 13 for previous work in a quasiperiodic system).

Ultracold atom gases confined in disordered potentials have recently emerged as an ideal system for exploring these fundamental questions^{1,2,14}. Disorder can be controllably introduced using an optical speckle field^{15–18}; the disorder strength can be continuously varied by changing the optical intensity and precise characterization of the disordering potential is possible using high-resolution microscopy. Because the interactions between atoms can also be manipulated, the effects of disorder can be explored both in the non-interacting regime and in the strongly correlated limit. For example, Anderson localization in a disordered potential generated by speckle¹⁹ and in a quasicrystalline system²⁰ has been observed, and we have realized the DBH model in the strongly interacting regime by combining optical speckle with a three-dimensional optical lattice⁴.

In our experiment, ⁸⁷Rb Bose-Einstein condensates are confined in a disordered optical lattice created by three pairs of 812 nm laser beams and an optical speckle field produced using a 532 nm laser, as described in ref. 4. The bottom inset to Fig. 1 shows the

geometry of the lattice beams (red lines) and disordering potential (green arrow) projected onto the plane used to image the atom gas. We control the ratio of interaction energy U to tunnelling energy t for the atoms by tuning the lattice potential depth, which is characterized by a dimensionless parameter s (the lattice potential depth is sE_R along each lattice direction, where E_R is the atomic recoil energy—see Methods). Because the disorder in our experiment is fine grained (that is, smaller than two 406 nm lattice spacings along any lattice direction), the speckle potential leads to a distribution of all Hubbard parameters (see ref. 4). We characterize the strength of the disorder Δ by the average potential shift from the speckle field, which is equivalent to the standard deviation of the site-occupation-energy distribution. In contrast to our previous work in the high-filling limit⁴, we adjust the atom number so that approximately one particle occupies each site (on average) in the centre of the lattice for all of the data reported here.

The effect of disorder on the transport properties of the gas is shown in Fig. 1. Data are shown for the centre-of-mass (COM) velocity of the gas along the transverse (v_T) and longitudinal (v_L) speckle directions immediately after an applied impulse for $\Delta = 0, 0.75$ and $3 E_R$ and for a range of lattice depths spanning the superfluid (SF) and Mott insulator (MI) regimes in a clean lattice ($s = 6$ – 19). The technique we employ here is a modification of that used in ref. 3, in which the dissipation for transport γ is probed by measuring the COM motion of the gas in the parabolic confining potential after applying a spatially uniform impulse. These data are taken in the regime in which the dominant dissipation mechanism in a clean lattice arises from quantum phase slips. We work primarily in the limit of an impulse that is rapid compared with the harmonic motion but not the dissipation rate. In this regime ($\gamma \gg 1/\tau \gg \omega$), $v = (F\tau/m^*)e^{-\gamma\tau}$, where F is the force during the impulse of duration τ , ω is the oscillator frequency for motion in the parabolic potential and m^* is the effective mass (which depends on s). As we fix the impulse $F\tau$ for the data in Fig. 1, the emergence of an insulator at fixed s is characterized by $\gamma \rightarrow \infty$ and $v = 0$, which is denoted by the dashed line.

In the clean lattice, the velocity approaches zero as expected for an insulator when the potential depth is increased into the regime for which atoms in the unit-filling MI state exist in the centre of the lattice. This suppression of the COM velocity for increasing s is caused by an increase in effective mass (characterized by the prediction for $\gamma = 0$, which is shown by the solid black line) and by an enhancement in the quantum phase slip rate (which scales as $\gamma \propto e^{\sqrt{U}t}$). The atom gas does not completely transform into an insulator when atoms emerge in the MI state because an SF shell exists at the periphery of the gas at low temperature²¹; the signature of this SF is the finite condensate fraction N_0/N (defined as in ref. 4) observed for $s > 13.3$.

Although disorder weakly affects transport in the SF regime for $\Delta = 0.75 E_R$, increasing the disorder strength to $\Delta = 3 E_R$ transforms the SF state to an insulator (indicated by the vertical green

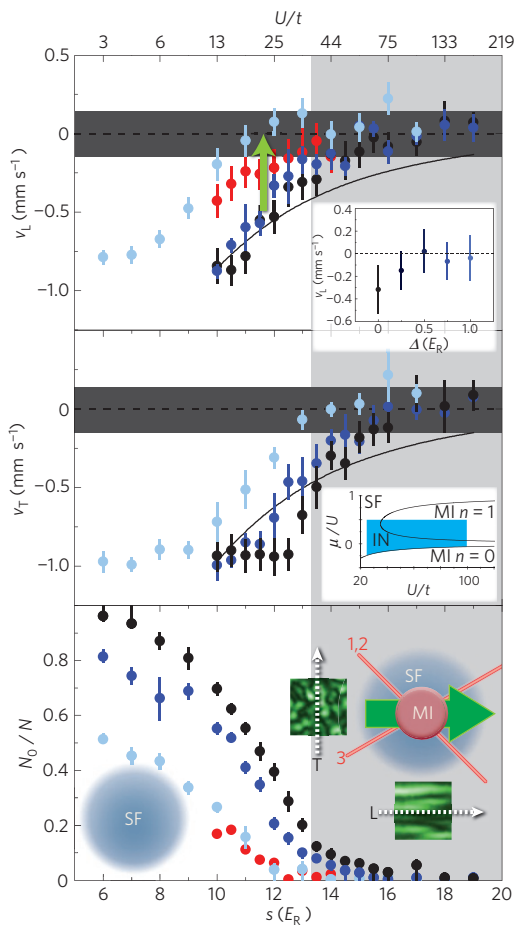


Figure 1 | Effect of disorder on transport. The overall COM velocity v of the gas after an impulse is applied as the lattice depth s is varied for three disorder strengths: $\Delta = 0$ (black), 0.75 (dark blue) and $3.0 E_R$ (light blue); data are shown for the longitudinal (top) and transverse (middle) directions. Data are also shown for high-temperature transport in a clean lattice (red); according to a site-decoupled mean-field theory²⁷ the temperature for these data ranges from 15 nK at $s = 10$ to 6 nK at $s = 14$. The top inset shows how disorder affects v_L for $s = 14$; the colour scale for the points follows the main figure for reference. Sample slices through the measured speckle-intensity profile are shown in the bottom inset along with the experimental geometry; the autocorrelation of speckle potential is cylindrically symmetric with characteristic speckle sizes 570 nm and $3 \mu\text{m}$ along the transverse and longitudinal directions to propagation. Within the region marked in light grey, a spherical core of unit-filling MI exists in the centre of the clean lattice (according to three-dimensional mean-field theory). The dark-grey band indicates the systematic uncertainty in determining zero velocity (see Methods). The error bars represent the statistical uncertainty in the (typically) seven measurements averaged for each point. The error bars for v also include the statistical uncertainty in determining zero velocity, and the error bars for N_0/N include a systematic error that reflects our inability to measure condensate fraction above 95% and below 5%.

arrow) at approximately $s = 12$, corresponding to $U/t = 25$ and $\Delta/t = 250$. This transition agrees within our systematic uncertainty (see Methods) in U/t and t with the prediction for an SF–Bose-glass phase boundary from recent quantum Monte Carlo work⁵. Measurements of the excitation spectrum and compressibility²² will be required before this insulator can be identified conclusively as a Bose glass. Within the systematic uncertainty in determining zero velocity (see Methods), the superfluid-to-insulator (SF–IN) transition occurs at the same s for the longitudinal and transverse

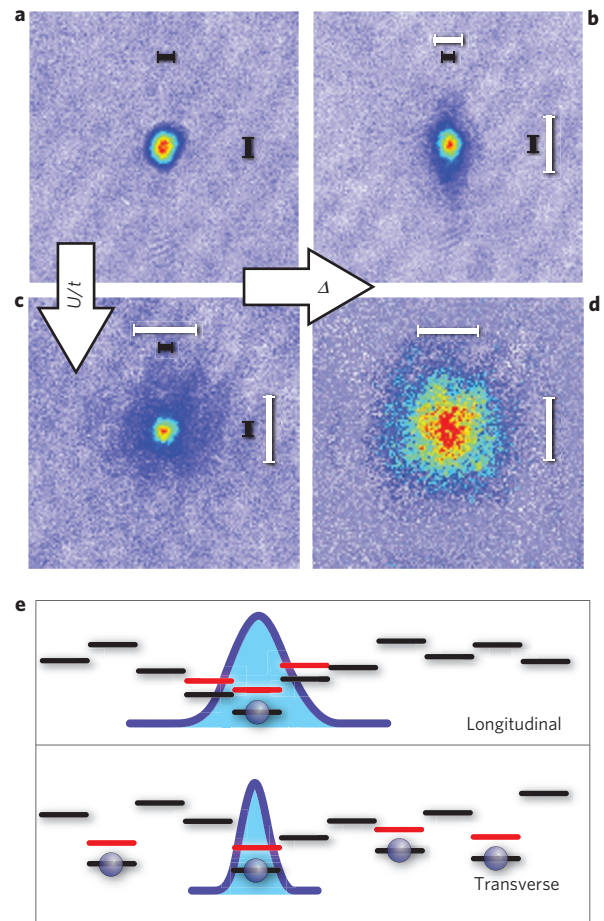


Figure 2 | Effect of disorder on atomic quasimomentum distribution. **a–d**, Images taken after band-mapping from the disordered lattice and TOF are shown in false colour for $s = 6$, $\Delta = 0$ (**a**), $s = 6$, $\Delta = 3 E_R$ (**b**), $s = 12$, $\Delta = 0$ (**c**) and $s = 12$, $\Delta = 3 E_R$ (**d**). The TOF is 25 ms for $s = 6$ and 15 ms for $s = 12$; the field of view for each image is 0.6 mm. The images are fitted to two-component Gaussian distributions to determine condensate fraction and the sizes and locations of the condensate and NC. The black and white bars correspond to twice the fitted r.m.s. radius for the condensate and NC components. **e**, A simple model—suggested by the behaviour in **b**—that may be used to understand the effect of disorder on the quasimomentum distribution. Atoms (blue spheres) localize to regions (blue curves) to screen the disordered potential and create a more uniform effective potential.

directions. The region of U/t and effective chemical potential μ that we determine as insulating is shown superimposed in blue on the phase diagram for the clean system in the middle inset to Fig. 1. Because of the confining harmonic potential, we sample a range of fillings and corresponding μ —we assume that the gas must be globally insulating for v to vanish after the impulse. This insulating region is consistent with an early, qualitative prediction for the DBH phase diagram²³. The plot of N_0/N for $\Delta = 0$, 0.75 and $3 E_R$ in Fig. 1 shows that the emergence of the disordered insulating state coincides with the obliteration of the condensate by disorder. To assess the impact of finite temperature, we measure the transport properties for atoms in the clean lattice ($\Delta = 0 E_R$) at sufficiently high temperature to match the condensate fraction observed at $\Delta = 3 E_R$. Even though at this temperature the entropy per particle in the clean lattice is higher than for $\Delta = 3 E_R$ (see the discussion that follows), the gas is not insulating, therefore indicating that the observed SF–IN transition is not caused exclusively by heating introduced by the speckle field.

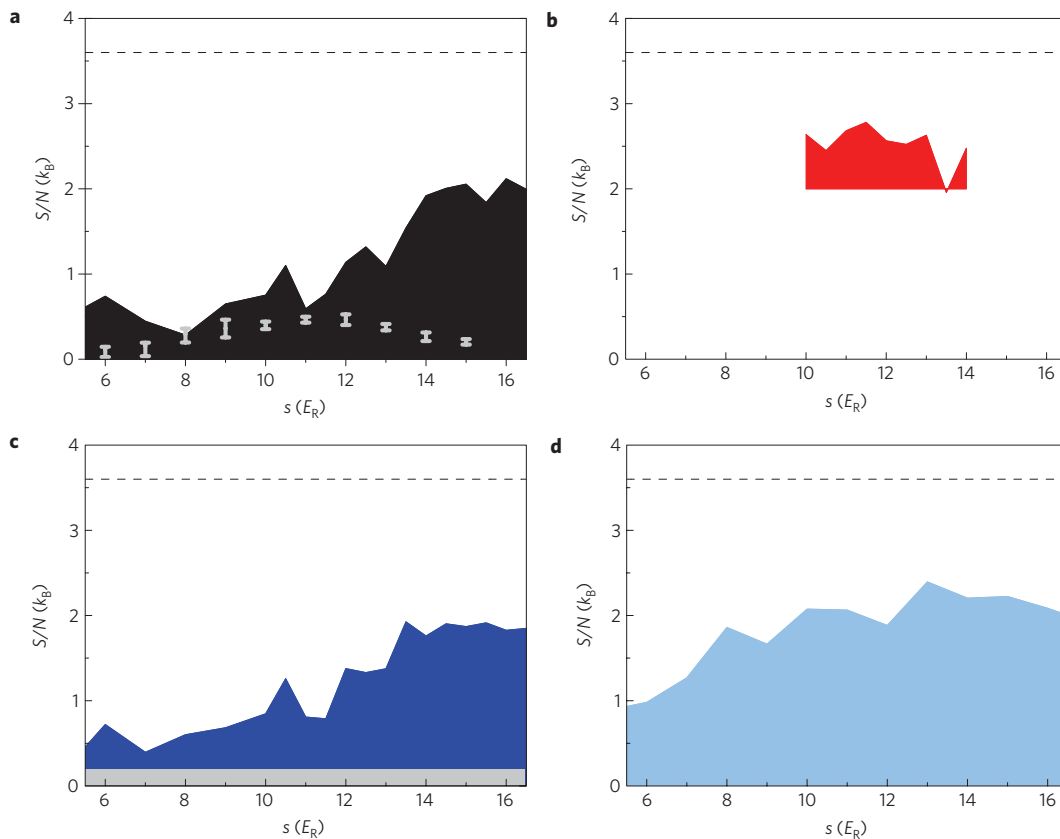


Figure 3 | Bounds on entropy per particle. **a–d**, The entropy per particle S/N is determined to lie within the coloured regions for $\Delta = 0 E_R$ (black, **a**), $\Delta = 0 E_R$ at high temperature (red, **b**), $\Delta = 0.75 E_R$ (dark blue, **c**) and $\Delta = 3.0 E_R$ (light blue, **d**). The S/N corresponding to the critical temperature for condensation in a weakly interacting, parabolically confined system is indicated by the dashed black line. The systematic uncertainty in the lower bound related to our inability to resolve high N_0/N is shown by the light-grey band in **c**. There is typically both a $0.2 k_B$ systematic and $0.2 k_B$ statistical uncertainty in the upper bound. The minor, disorder-induced heating implied by the increase in the upper bound for $\Delta = 3 E_R$ between $s = 8$ and 11 may be an artefact of the measurement technique. For comparison, we find that the S/N determined from band-mapped N_0/N measured in the clean lattice (light-grey points) is close to the lower bound for all s , even though the upper bound increases significantly for $s > 12$. We calculate S/N for these points using the local density approximation and site-decoupled mean-field theory to self-consistently solve for the temperature and chemical potential²⁷; the error bars shown in the figure represent the statistical uncertainty from the spread in the measured N_0/N used to determine S/N .

Some hints about the mechanism behind the extraordinary robustness of superfluidity in this system are revealed in representative images (shown in Fig. 2) of the atomic quasimomentum distribution taken after band-mapping²⁴ (see Methods) and time of flight (TOF). The transition to an insulator at $s = 12$ for $\Delta = 3$ is marked by dramatic, but not unexpected, behaviour: the condensate is destroyed, giving rise to a broad quasimomentum distribution (Fig. 2d). The quasimomentum distribution in Fig. 2d closely resembles the distribution deep in the MI regime, in which the atoms have equal quantum amplitude at all quasimomenta and are therefore localized, as anticipated for an insulator.

More informative is the effect of disorder observed at $s = 6$, well into the SF regime of the clean BH model. The non-condensate (NC) populated by applying strong disorder ($\Delta = 3 E_R$) reflects the symmetry of the speckle field, with a diameter approximately twice as large along the transverse direction (Fig. 2b). This behaviour directly confirms a conjecture that atoms can localize to screen the disorder through interactions^{6,25,26}. A random distribution of site energies—indicated by black lines in Fig. 2e—would result in high-kinetic-energy states localized into the deepest lattice wells for non-interacting particles. The strong repulsive interactions present in this many-particle system, however, prevent multiple occupation of these localized states. Instead, only a fraction of the atoms localize into the deepest wells, leading to a corresponding reduction of condensate fraction. The remaining atoms exist in a

delocalized, lower-energy SF state because they experience a more uniform effective potential (red lines in Fig. 2e) arising from their interactions with the localized atoms. The asymmetry of the NC at $s = 6$ is a direct result of the difference in speckle correlation-length scales along the transverse and longitudinal directions: in contrast to the transverse direction, for which energy shifts are uncorrelated from site to site, the atoms can localize to a several-site region to screen the disorder along the longitudinal direction.

In contrast to many theoretical predictions for the DBH model, which exhibit a re-entrant superfluid (RSF) generated by introducing disorder to an MI (refs 7–10), we find that increasing disorder generically leads to larger dissipation. To directly test for an RSF, we measure transport as Δ is varied at $s = 14$ ($U/t = 44$), for which approximately half of the atoms start in the MI phase in the clean lattice at zero temperature (according to the local density approximation and site-decoupled mean-field theory²⁷). The data shown in the top inset to Fig. 1 are typical for all lattice depths: increasing Δ leads to greater dissipation (and corresponding decrease in $|\nu|$) for motion along either the longitudinal or transverse directions. This behaviour is in conflict with, for example, ref. 7, which predicts that the gas should wholly convert into an SF at $U/t \approx 40$ for this range of disorder, and hence that the dissipation strength should decrease.

The conspicuous absence of the RSF in this system may be the result of several factors, such as finite system size, non-zero

temperature and the microscopic disorder parameters for our system, none of which (to our knowledge) have been included in a complete theoretical treatment. Although finite-size effects have been found to impact the MI phase boundaries²⁸, the RSF is present in numerical simulations with lattices smaller than those sampled here⁹. Furthermore, this phase has been discovered in theoretical treatments for a variety of disorder distributions. Therefore, we feel that the most probable explanation for this discrepancy is finite temperature, because there is evidence that the RSF has an exceptionally low critical temperature⁵. Unfortunately, we cannot measure temperature precisely because there is not a quantitative, verified theory that connects measurable quantities to temperature.

We have therefore measured bounds on entropy per particle S/N to constrain future finite-temperature theoretical treatments. To determine the limits shown in Fig. 3, we measure condensate fraction in the purely parabolic potential before transferring the atoms into the disordered lattice and after slowly turning off the lattice. The second law of thermodynamics ensures that this procedure provides lower and upper bounds on entropy. The entropy per particle is determined using $S/N = 3.6(1 - N_0/N)$, which is exact for a non-interacting gas and approximately correct for an interacting, harmonically trapped gas for the range of N_0/N measured here²⁹. For the RSF regime, we find that $S/N < 2k_B$, where k_B is Boltzmann's constant.

Methods

We create ⁸⁷Rb Bose–Einstein condensates using a hybrid magneto-optical trap that is generated using a magnetic quadrupole field and a 1,064 nm focused laser beam (see ref. 24 for details); the geometric mean of the trap frequencies (without the lattice) is 40 Hz. $E_R = \hbar^2/2m\lambda^2$, where \hbar is Planck's constant, m is the atomic mass and $\lambda = 812$ nm is the wavelength of the light used to create the lattice. The average number of atoms is $12 \pm 4 \times 10^3$, corresponding to 1.4 and 1 particles per site in the centre of the clean lattice for $s = 6$ and 14 according to site-decoupled mean-field theory and the local density approximation. The ratio U/t is calculated from s using a band-structure calculation and the known atomic-interaction parameters. Our typical systematic uncertainty in s is 6%, which corresponds to 25% in U/t and 12% in t at $s = 12$, for example.

An impulse is applied along the transverse direction by translating the 1,064 nm laser beam by 7 μ m using a 3 ms trapezoidal ramp. A uniform magnetic field is applied for 1 ms to create a longitudinal impulse. The magnitude and timing of the magnetic-field pulse and the laser-beam displacement were adjusted to produce approximately equal impulses along the two directions. We turn off the disordered lattice after the impulse using a 200 μ s linear ramp of the lattice and speckle light. The impulse does not significantly affect the condensate fraction measured after TOF.

The systematic uncertainty in determining zero velocity arises from using a technique that is unbiased but can result in positive v , which is unphysical given the fixed impulse direction. We set zero velocity by measuring the COM position x_0 of the NC without an applied impulse. We correct for a systematic shift in x_0 that depends on Δ arising from a slight misalignment of the speckle field with respect to the centre of the lattice. We also observe a weak systematic dependence of x_0 on s . The ± 0.15 mm s⁻¹ systematic uncertainty shown in Fig. 3 is equivalent to the spread in x_0 for all s and Δ used in this work. The measured velocity of the condensate and NC components after the impulse is determined by the displacement from x_0 following 20 ms TOF. The COM velocity is defined as $v = (v_0 N_0 / (N_{NC} + v_{NC}) + N_0 / N_{NC}) / (1 + N_0 / N_{NC})$, where v_0 and v_{NC} are the condensate and NC velocities, and N_0 and N_{NC} are the numbers of condensate and NC atoms.

Received 28 December 2009; accepted 11 June 2010;
published online 18 July 2010

References

- Lewenstein, M. *et al.* Ultracold atomic gases in optical lattices: Mimicking condensed matter physics and beyond. *Adv. Phys.* **56**, 243–379 (2007).
- Sanchez-Palencia, L. & Lewenstein, M. Disordered quantum gases under control. *Nature Phys.* **6**, 87–95 (2010).
- McKay, D., White, M., Pasienski, M. & DeMarco, B. Phase-slip-induced dissipation in an atomic Bose–Hubbard system. *Nature* **453**, 76–79 (2008).

- White, M. *et al.* Strongly interacting bosons in a disordered optical lattice. *Phys. Rev. Lett.* **102**, 055301 (2009).
- Gurarie, V., Pollet, L., Prokof'ev, N. V., Svistunov, B. V. & Troyer, M. Phase diagram of the disordered Bose–Hubbard model. *Phys. Rev. B* **80**, 214519 (2009).
- Trivedi, N. in *Proc. of the 20th International Workshop on Condensed Matter Theories* Vol. 12 141–157 (Plenum Press, 1997).
- Bissbort, U. & Hofstetter, W. Stochastic mean-field theory for the disordered Bose–Hubbard model. *Europhys. Lett.* **86**, 50007 (2009).
- Wu, J. & Phillips, P. Minimal model for disorder-induced missing moment of inertia in solid ⁴He. *Phys. Rev. B* **78**, 014515 (2008).
- Pollet, L., Prokof'ev, N. V., Svistunov, B. V. & Troyer, M. Absence of a direct superfluid to Mott insulator transition in disordered Bose systems. *Phys. Rev. Lett.* **103**, 140402 (2009).
- Kruger, F., Wu, J. & Phillips, P. Anomalous suppression of the Bose glass at commensurate fillings in the disordered Bose–Hubbard model. *Phys. Rev. B* **80**, 094526 (2009).
- Giamarchi, T. & Schulz, H. J. Localization and interaction in one-dimensional quantum fluids. *Europhys. Lett.* **3**, 1287–1293 (1987).
- Fallani, L., Lye, J. E., Guarrera, V., Fort, C. & Inguscio, M. Ultracold atoms in a disordered crystal of light: Towards a Bose glass. *Phys. Rev. Lett.* **98**, 130404 (2007).
- Roscilde, T. Bosons in one-dimensional incommensurate superlattices. *Phys. Rev. A* **77**, 063605 (2008).
- Damski, B., Zakrzewski, J., Santos, L., Zoller, P. & Lewenstein, M. Atomic Bose and Anderson glasses in optical lattices. *Phys. Rev. Lett.* **91**, 080403 (2003).
- Lye, J. E. *et al.* Bose–Einstein condensate in a random potential. *Phys. Rev. Lett.* **95**, 070401 (2005).
- Chen, Y. P. *et al.* Phase coherence and superfluid–insulator transition in a disordered Bose–Einstein condensate. *Phys. Rev. A* **77**, 033632 (2008).
- Clement, D. *et al.* Suppression of transport of an interacting elongated Bose–Einstein condensate in a random potential. *Phys. Rev. Lett.* **95**, 170409 (2005).
- Schulte, T. *et al.* Routes towards Anderson-like localization of Bose–Einstein condensates in disordered optical lattices. *Phys. Rev. Lett.* **95**, 170411 (2005).
- Billy, J. *et al.* Direct observation of Anderson localization of matter waves in a controlled disorder. *Nature* **453**, 891–894 (2008).
- Roati, G. *et al.* Anderson localization of a non-interacting Bose–Einstein condensate. *Nature* **453**, 895–898 (2008).
- DeMarco, B., Lannert, C., Vishveshwara, S. & Wei, T.-C. Structure and stability of Mott–insulator shells of bosons trapped in an optical lattice. *Phys. Rev. A* **71**, 063601 (2005).
- Delande, D. & Zakrzewski, J. Compression as a tool to detect Bose glass in a cold atomic gas. *Phys. Rev. Lett.* **102**, 085301 (2009).
- Fisher, M. P., Weichman, P. B., Grinstein, G. & Fisher, D. S. Boson localization and the superfluid–insulator transition. *Phys. Rev. B* **40**, 546–570 (1989).
- McKay, D., White, M. & DeMarco, B. Lattice thermodynamics for ultra-cold atoms. *Phys. Rev. A* **79**, 063605 (2009).
- Krauth, W., Trivedi, N. & Ceperley, D. Superfluid–insulator transition in disordered boson systems. *Phys. Rev. Lett.* **67**, 2307–2310 (1991).
- Scalettar, R. T., Batrouni, G. G. & Zimanyi, G. T. Localization in interacting, disordered, Bose systems. *Phys. Rev. Lett.* **66**, 3144–3147 (1991).
- Lu, X. & Yu, Y. Finite-temperature effects on the number fluctuation of ultracold atoms across the superfluid-to-Mott-insulator transition. *Phys. Rev. A* **74**, 063615 (2006).
- Freericks, J. K. & Monien, H. Strong-coupling expansions for the pure and disordered Bose–Hubbard model. *Phys. Rev. B* **53**, 2691–2700 (1996).
- Catani, J. *et al.* Entropy exchange in a mixture of ultracold atoms. *Phys. Rev. Lett.* **103**, 140401 (2009).

Acknowledgements

This work was supported by the DARPA OLE program (ARO award W911NF-08-1-0021), the Sloan Foundation and the National Science Foundation (award 0448354). D.M. acknowledges support from NSERC.

Author contributions

M.P., M.W., D.M. and B.D. conceived and designed the experiments. M.P., D.M. and B.D. analysed the data, which were acquired by M.P.

Additional information

The authors declare no competing financial interests. Reprints and permissions information is available online at <http://npg.nature.com/reprintsandpermissions>. Correspondence and requests for materials should be addressed to B.D.